

# Microwave and Quantum Chemical Study of Propa-1,2-dienyl Thiocyanate ( $\text{H}_2\text{C}=\text{C}=\text{CHSC}\equiv\text{N}$ )

Harald Møllendal,<sup>\*,†</sup> George C. Cole,<sup>†</sup> and Jean-Claude Guillemin<sup>‡</sup>

Department of Chemistry, University of Oslo, Post Office Box 1033 Blindern, NO-0315 Oslo, Norway, and Sciences Chimiques de Rennes, UMR 6226 CNRS-ENSCR, Ecole Nationale Supérieure de Chimie de Rennes F-35700 Rennes, France

Received: December 18, 2006; In Final Form: January 23, 2007

The microwave spectrum of propa-1,2-dienyl thiocyanate ( $\text{H}_2\text{C}=\text{C}=\text{CHSC}\equiv\text{N}$ ) has been investigated in the 24–40 and 50–80 GHz spectral regions. The spectrum of one conformer was assigned. This rotamer, which has a C–C–S–C dihedral angle of about  $134^\circ$  from synperiplanar, is at least 2 kJ/mol more stable than any other form. Two vibrationally excited states assumed to belong to the first excited state of the C–S torsional vibration and to a low bending mode were assigned. Their frequencies were determined to be 62(20) and 155(30)  $\text{cm}^{-1}$ , respectively. The microwave work has been augmented by ab initio calculations at the MP2/aug-cc-pVTZ and density functional theory calculations at the B3LYP/aug-cc-pVTZ level of theory. The B3LYP calculations are generally in better agreement with the observations than the MP2 calculations.

## Introduction

Organic thiocyanates,  $\text{RSC}\equiv\text{N}$ , have a C–S–C angle of approximately  $100^\circ$  and may therefore exist in different conformations, owing to restricted rotation about the R–S bond. Relatively few gas-phase studies of the conformational properties of thiocyanates have been reported. Ethylthiocyanate ( $\text{CH}_3\text{CH}_2\text{SCN}$ ) has been studied by microwave (MW)<sup>1</sup> spectroscopy in the gas phase and by infrared (IR) spectroscopy using the matrix-isolation technique.<sup>2</sup> The C–C–S–C dihedral angle determines the conformation of this compound. Only the synclinal, *sc*, conformer, in which this angle is  $58^\circ$  from synperiplanar, *sp* ( $0^\circ$ ), was identified in the MW work.<sup>1</sup> The antiperiplanar, *ap*, rotamer, where the C–C–S–C dihedral angle is  $180^\circ$  from *sp*, was identified in the matrix-isolation study in addition to the *sc* form.<sup>2</sup> The *sc* rotamer was determined to be 4.2(3) kJ/mol more stable than the *ap* conformer.<sup>2</sup>

Propargyl thiocyanate ( $\text{H}-\text{C}\equiv\text{C}-\text{CH}_2\text{SCN}$ ) has been investigated by infrared and Raman spectroscopies and gas electron diffraction.<sup>3</sup> It was found that this compound exists as a mixture of two forms, a less stable C–C–S–C *sc* form and a more stable *ap* conformer. The electron-diffraction  $r_\alpha$  values for the C–C–S–C dihedral angle were  $57(8)^\circ$  for the *sc* conformer and  $171(12)^\circ$  for the *ap* form. The energy difference was determined to be 1.24 kJ/mol with the *ap* rotamer as the more stable.<sup>3</sup>

Two rotamers, *ap* and *sc*, exist for isopropyl thiocyanate ( $\text{CH}_3\text{CH}(\text{SCN})\text{CH}_3$ ) according to an infrared and Raman study.<sup>4</sup> The *ap* form is the more stable in this case; the enthalpy difference in the gas phase was found to be 2.3(3) kJ/mol using matrix-isolation techniques.<sup>4</sup>

Ethenyl thiocyanate ( $\text{H}_2\text{C}=\text{CHSCN}$ ) has been studied by MW, Raman, and infrared spectroscopies.<sup>5,6</sup> This compound has a more stable *sp* form (C–C–S–C dihedral angle =  $0^\circ$ ) and a

less stable anticlinal, *ac*, rotamer, where this angle is approximately  $130^\circ$  from *sp*.<sup>5,6</sup> The energy difference is 3–6 kJ/mol in the gas, according to the MW study.<sup>5,6</sup>

These examples show that the conformational properties of thiocyanates are very sensitive to the groups to which the thiocyanate group is attached. In the title compound, propa-1,2-dienyl thiocyanate ( $\text{H}_2\text{C}=\text{C}=\text{CHSCN}$ ), henceforth called PDT, the thiocyanate group is adjacent to the allenyl group. The fact that no conformational studies have previously been performed for compounds in which the thiocyanate group is adjacent to an allenyl group motivated the present investigation.

The methods we have used are MW spectroscopy and high-level quantum chemical calculations. MW spectroscopy was chosen because of its high accuracy and resolution, making this method especially suitable for conformational studies. The spectroscopic work has been augmented by high-level quantum chemical calculations, which were conducted with the purpose of obtaining information for use in assigning the MW spectrum and investigating properties of the potential energy hypersurface.

## Experimental Section

**Synthesis of Propa-1,2-dienyl Thiocyanate.** Two syntheses of propa-1,2-dienyl thiocyanate have been reported.<sup>7,8</sup> The first preparation involved the synthesis of thiocyanogen followed by its reaction with triphenyl-2-propynylstannane.<sup>9</sup> In the second, flash vacuum pyrolysis of 3-isothiocyano-1-propyne gave a mixture of the starting material and propa-1,2-dienyl thiocyanate.<sup>8</sup> To prepare a pure sample, we modified the approach of Bullpitt and Kitching.<sup>7</sup>

In a two-necked flask equipped with a stirring bar and a nitrogen inlet were introduced lead(II) thiocyanate (2.50 g, 7.7 mmol) and benzene (20 mL).<sup>10</sup> The flask was immersed in a cold bath ( $5^\circ\text{C}$ ), and dibromine (1.23 g, 7.7 mmol) in benzene (10 mL) was added dropwise. The reaction mixture was then stirred at room temperature for 30 min. The mixture was filtered under nitrogen, and the clear solution was slowly introduced in another two-necked flask containing a cooled solution ( $5^\circ\text{C}$ ) of triphenyl-2-propynylstannane (2.0 g, 5.1 mmol) in benzene

\* To whom correspondence should be addressed. E-mail: harald.mollendal@kjemi.uio.no.

<sup>†</sup> University of Oslo.

<sup>‡</sup> Ecole Nationale Supérieure de Chimie de Rennes.

(20 mL). The mixture was stirred for 2 h at room temperature, and water (5 mL) was added. The reaction mixture was taken up in diethyl ether/water ( $3 \times 20$  mL). The organic phases were combined and dried over  $\text{MgSO}_4$ . After filtration, most of the solvent was removed under vacuum. The flask containing the crude solution was then attached to a vacuum line equipped with a trap immersed in a bath cooled at  $-20^\circ\text{C}$ . The low-boiling compounds were distilled and the flask was heated up to  $60^\circ\text{C}$ . Propa-1,2-dienyl thiocyanate (0.38 g, 3.9 mmol) was selectively trapped in the cold trap. A very pure product can be obtained after a second distillation. Yield: 76% (based on triphenyl-2-propynylstannane).  $\text{bp}_{0.1}$   $30^\circ\text{C}$ .  $^1\text{H}$  NMR ( $\text{CDCl}_3$ , 400 MHz)  $\delta$  5.30 (d, 2H,  $^3J_{\text{HH}} = 6.1$  Hz,  $\text{CH}_2$ ); 5.83 (t, 1H,  $^3J_{\text{HH}} = 6.1$  Hz, CH).  $^{13}\text{C}$  NMR ( $\text{CDCl}_3$ , 100 MHz)  $\delta$  78.0 (d,  $^1J_{\text{CH}} = 197.5$  Hz, CH); 82.5 (t,  $^1J_{\text{CH}} = 171.0$  Hz,  $\text{CH}_2$ ); 110.0 (s, CN); 209.2 (s,  $\text{C}=\text{C}=\text{C}$ ).

**Microwave Experiment.** The MW spectrum was recorded in the 24–40 and 50–80 GHz spectral regions using the Stark-modulated spectrometer of the University of Oslo. Individual transitions were measured with an estimated accuracy of  $\approx 0.15$  MHz. Details of the construction and operation of this device, which has a 2 m Hewlett-Packard Stark cell, have been given elsewhere.<sup>11,12</sup> The cell was cooled to roughly  $-10^\circ\text{C}$  while recording the spectrum in the 24–40 GHz region in order to enhance the intensity of the spectral lines. Lower temperatures, which would have increased the intensity of the spectrum even more, could not be achieved, owing to insufficient vapor pressure of PDT. The spectrum in the 50–80 GHz is considerably stronger than at lower frequencies and was therefore recorded at room temperature. Radio frequency microwave double resonance experiments (RFMWDR), similar to those performed by Wodarczyk and Wilson,<sup>13</sup> were also conducted to assign unambiguously particular transitions.

## Results

**Quantum Chemical Calculations.** The present ab initio and density functional theory (DFT) calculations were performed employing the Gaussian 03 suite of programs,<sup>14</sup> running on the 64 processor HP “superdome” computer in Oslo. Electron correlation was taken into consideration in the ab initio calculations using the Møller–Plesset second-order perturbation calculations (MP2).<sup>15</sup> Becke’s three-parameter hybrid functional<sup>16</sup> employing the Lee, Yang, and Parr correlation functional<sup>17</sup> (B3LYP) was employed in the DFT calculations. Dunning’s<sup>18</sup> correlation-consistent triple- $\zeta$  basis set, aug-cc-pVTZ, which includes polarized functions for the valence electrons and is augmented by additional diffuse functions, was used throughout this work.

Rotation about the C5–S6 bond (Figure 1) produces rotational isomerism for PDT. Two typical forms, denoted *sp* and *ac*, where the C2–C5–S6–C8 dihedral angle are  $0^\circ$  (*sp*) and approximately  $130^\circ$  (*ac*), respectively, are sketched in Figure 1. B3LYP/aug-cc-pVTZ calculations of the energies were first performed for the  $0^\circ$ – $180^\circ$  interval in steps of  $10^\circ$  of the C2–C5–S6–C8 dihedral angle, employing the scan option of the Gaussian 03 program, allowing all remaining structural parameters to vary freely. The resulting potential function indicated that there are two minima (two “stable” conformers) of the potential energy hypersurface, at about  $0^\circ$  and  $135^\circ$  for the C2–C5–S6–C8 dihedral angle.

Separate B3LYP calculations of the energies and vibrational frequencies were made next for these two rotamers in order to locate the exact values of the energies and geometries of the *sp* and *ac* rotamers. The starting values of the C2–C5–S6–C8

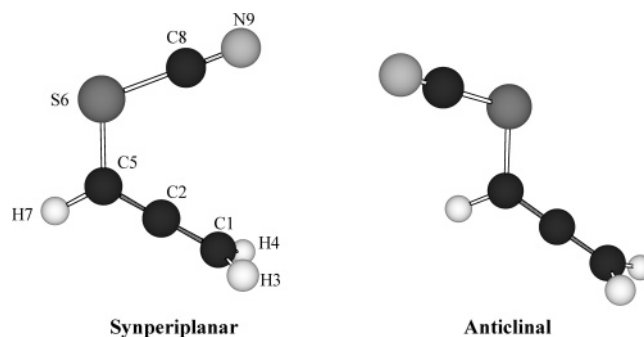


**Figure 1.** Synperiplanar (*sp*) and anticlinal (*ac*) forms of  $\text{H}_2\text{C}=\text{C}=\text{CHSCN}$  with atom numbering. The MW spectrum of the *ac* rotamer was assigned. This rotamer is at least 2 kJ/mol more stable than the *sp* conformer.

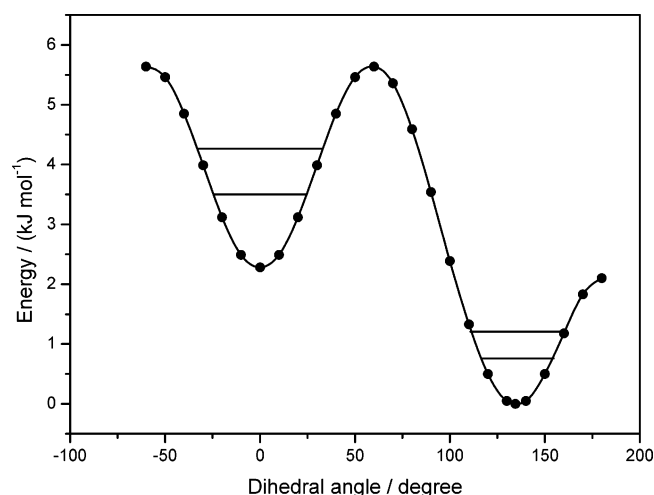


**Figure 2.** B3LYP/aug-cc-pVTZ potential function for rotation about the C5–S6 bond. The values of the C2–C5–S6–C8 dihedral angle are given on the abscissa. A dihedral angle of  $0^\circ$  corresponds to the *sp* conformer, and a dihedral angle of  $134.4^\circ$  corresponds to the *ac* rotamer. The ground vibrational and the first excited C5–S6 torsional states of the *sp* and *ac* forms are indicated as horizontal lines on this plot.

dihedral angles were chosen to be close to  $0^\circ$  and  $135^\circ$ , respectively. Full geometry optimizations with no symmetry restrictions were carried out employing the default convergence criteria of Gaussian 03. The *sp* conformer was found to have a symmetry plane ( $C_s$  symmetry), the said dihedral angle being exactly  $0^\circ$ . The C2–C5–S6–C8 dihedral angle was found to be  $134.4^\circ$  in the *ac* rotamer. Only positive values were found for the vibrational frequencies, as expected for these two minima on the potential energy hypersurface.

MP2 calculations were repeated for the *sp* and *ac* rotamers. The *sp* form was again found to have exact  $C_s$  symmetry, whereas the C2–C5–S6–C8 dihedral angle was predicted to be  $129.6^\circ$  in the *ac* conformer.

It is possible to construct a potential energy function (shown in Figure 2) based on the B3LYP results. The maxima of this function are found at a value of  $60^\circ$  for the C2–C5–S6–C8 dihedral angle, 5.6 kJ/mol above the energy of the *ac* rotamer, and at  $180^\circ$ , 2.1 kJ/mol above the minimum energy. The uncorrected C5–S6 torsional frequencies, which were  $65.3\text{ cm}^{-1}$  for the *sp* and  $39.6\text{ cm}^{-1}$  for *ac* conformers, are indicated as horizontal lines on this plot. The MP2 results for these uncorrected frequencies were  $72.2$  and  $39.1\text{ cm}^{-1}$ , respectively.

The MP2 and B3LYP geometries are listed in Table 1, while additional parameters obtained in these calculations are displayed in Table 2. It can be seen from Table 1 that the MP2 and B3LYP bond lengths agree to within about 1 pm, with the

**TABLE 1: MP2 and B3LYP Geometries<sup>a,b</sup> of the *sp* and *ac* Conformers of H<sub>2</sub>C=C=CHSCN**

method conformer	MP2 <i>sp</i>	MP2 <i>ac</i>	B3LYP <i>sp</i>	B3LYP <i>ac</i>
bond length (pm)				
C1–C2	130.9	130.8	129.9	129.8
C1–H3	108.2	108.2	108.4	108.3
C1–H4	108.2	108.2	108.4	108.3
C2–C5	130.5	130.8	129.7	129.9
C5–S6	178.8	178.3	179.3	179.1
C5–H7	108.2	108.2	108.3	108.2
S6–C8	168.7	169.5	168.6	169.2
C8–N9	117.8	117.8	115.6	115.6
angle (deg)				
C2–C1–H3	120.8	120.6	121.3	121.1
C2–C1–H4	120.8	120.8	121.3	121.4
H3–C1–H4	118.4	118.6	117.3	117.5
C2–C5–S6	124.6	119.6	126.8	120.4
C2–C5–H7	123.5	123.2	123.2	123.2
S6–C5–H7	111.8	117.0	110.0	116.2
C5–S6–C8	98.8	98.1	101.8	100.2
C1–C2–C5	177.8	179.4	179.3	179.4
S5–C8–N9	179.2	178.3	177.2	177.4
dihedral angle (deg)				
H3–C1–C5–S6	89.5	95.2	89.7	95.7
H3–C1–C5–H7	–90.5	–90.2	–90.3	–90.0
H4–C1–C5–S6	–89.5	–84.8	–89.7	–84.6
H4–C1–C5–H7	90.5	89.8	90.3	90.9
C2–C5–S6–C8	0.0	–129.6	0.0	–134.4
H7–C5–S6–C8	180.0	55.0	180.0	51.6
C1–C2–C5–S6	–0.1	–47.3	0.3	–78.3
C5–S6–C8–N9	–179.8	–155.0	180.0	–163.1

<sup>a</sup> Basis set: aug-cc-pVTZ.<sup>18</sup> <sup>b</sup> Atom numbering is given in Figure 1.

**TABLE 2: MP2 and B3LYP<sup>a</sup> Rotational Constants, Centrifugal Distortion Constants, Dipole Moments, and Energy Differences between the *sp* and *ac* Conformers of H<sub>2</sub>C=C=CHSCN**

method conformer	MP2 <i>sp</i>	MP2 <i>ac</i>	B3LYP <i>sp</i>	B3LYP <i>ac</i>
rotational constants (MHz)				
A	4185.2	9032.1	4315.3	9987.0
B	2598.2	1440.1	2379.5	1393.9
C	1621.0	1322.3	1550.0	1291.9
centrifugal distortion constants <sup>b</sup> (kHz)				
$\Delta_J$	1.85	0.984	1.81	0.724
$\Delta_{JK}$	2.31	–42.2	–1.31	–40.1
$\Delta_K$	–2.65	650.	1.69	795.
$\delta_J$	0.713	0.178	0.707	0.0938
$\delta_K$	4.24	–6.79	3.32	–8.18
dipole moment components <sup>c</sup> (10 <sup>–30</sup> C m)				
$\mu_a$	6.2	15.8	7.6	15.2
$\mu_b$	10.4	4.0	9.5	3.4
$\mu_c$	0.0 <sup>d</sup>	1.4	0.0 <sup>d</sup>	1.5
$\mu_{\text{tot}}$	12.1	16.4	12.1	15.7
energy differences <sup>e</sup> (kJ/mol)				
$\Delta E$	0.0 <sup>f</sup>	2.3	2.2	0.0 <sup>g</sup>

<sup>a</sup> aug-cc-pVTZ basis set. <sup>b</sup> A-reduction.<sup>19</sup> <sup>c</sup> 1 debye = 3.33564 × 10<sup>–30</sup> C m. <sup>d</sup> For symmetry reasons. <sup>e</sup> Relative to lowest energy conformer corrected for zero-point vibrational energies. <sup>f</sup> Total MP2 energy corrected for zero-point vibrational energy: –1 591 403.4 kJ/mol. <sup>g</sup> Total B3LYP energy corrected for zero-point vibrational energy: –1 594 038.8 kJ/mol.

exception of the C8N9 triple bond, which is predicted to 2.2 pm shorter in the B3LYP than in the MP2 calculations. The bond angles associated with bonds between carbon atoms and hydrogen atoms are quite similar in the two calculations, whereas the bond angle involving the sulfur atom varies by up

to 3.3° (the C5–S6–C8 angle of the *sp* rotamer). There is also a difference of 3.7° in the C2–C5–S6–C8 dihedral angle of the *ac* rotamer.

The difference between the MP2 and B3LYP geometries results in variations in values of the rotational constants, which are especially large for the *A* rotational constant of the *ac* conformer (approximately 10% difference), as seen in Table 2. The A-reduction quartic centrifugal distortion constants<sup>19</sup> predicted by the two methods also differ considerably, whereas the dipole moment components vary by less than about 10% (Table 2).

Interestingly, the energy differences between the *ac* and *sp* conformers predicted in the two procedures vary. The MP2 calculations predict that the *sp* rotamer is favored by 2.3 kJ/mol over the *ac* form after corrections for zero-point vibrational energies, whereas the opposite result is obtained in the B3LYP calculations, where the *ac* form is calculated to be favored by 2.2 kJ/mol relative to the *sp* form (Table 2).

**Microwave Spectrum and Assignments.** The quantum chemical calculations above indicate that the rotational constants of the two forms are relatively small and that there are about five vibrational fundamentals with frequencies below 500 cm<sup>–1</sup> for each rotamer (not given in Table 1 or 2). The lowest vibrational frequency of each conformer is the C5–S6 torsional frequency, predicted to be in the 35–75 cm<sup>–1</sup> range (see above). PDT will consequently have a relatively large partition function, and each quantum state will therefore have a comparatively low population, resulting in a relatively weak MW spectrum. Cooling of the Stark cell reduces the partition function and enhances spectral intensities. It is unfortunate that PDT has a comparatively low vapor pressure, which makes it impossible to investigate the MW spectrum at lower temperatures than approximately –10 °C, using our equipment.

The MW spectrum of PDT turned out to be comparatively weak and dense, as expected. The lines were relatively broad owing to a large dipole moment and unresolved nuclear quadrupole hyperfine structure. This was the reason the spectral accuracy is no better than ±0.15 MHz.

The B3LYP calculations predict that the *ac* form is preferred, whereas the MP2 method predicts that the *sp* rotamer is more stable (Table 2). The *ac* form has its major dipole moment (≈15 × 10<sup>–30</sup> C m) along the *a*-principal inertial axis and the asymmetry parameter  $\kappa \approx -0.97$ . This rotamer was therefore expected to have a MW spectrum dominated by pileups of *a*-type R-branch transitions separated by  $B + C \approx 2.75$  GHz. The high-*K*<sub>–1</sub> members of these series are modulated at relatively low Stark voltages. Such pile-ups were readily observed when recording the spectrum in the 50–80 GHz region at a Stark voltage of about 50 V/cm. Detailed assignments of the individual <sup>a</sup>R-transitions were then performed. RFMWDR was used to confirm some of these assignments.

The *ac* conformer is predicted to have  $\mu_b \approx 4$  and  $\mu_c \approx 1 \times 10^{-30}$  C m, respectively (Table 2). *b*- and *c*-type transitions were therefore expected to be much less intense than the *a*-type lines are. The strongest lines of these categories were searched for but it was not possible to assign them unambiguously, presumably because of insufficient intensities.

The MW spectrum consisting of 244 <sup>a</sup>R-transitions of the ground vibrational state is given in the Supporting Information, Table 1S. The spectroscopic constants (A-reduction, *I*-representation<sup>19</sup>) derived from these lines in a least-squares fit are listed in Table 3. It was possible to determine only two quartic centrifugal distortion constants ( $\Delta_J$  and  $\Delta_{JK}$ ). The remaining quartic constants were preset at the values obtained



**TABLE 3: Spectroscopic Constants<sup>a</sup> of the Ground and Vibrationally Excited States of  $\text{H}_2\text{C}=\text{C}=\text{CHSCN}$** 

vibrational state	ground	first excited C–S torsion	low bending vibration
<i>A</i> (MHz)	9858.5(20)	9923.8(49)	10241.7(71)
<i>B</i> (MHz)	1415.6312(43)	1422.1436(64)	1407.502(12)
<i>C</i> (MHz)	1307.5570(41)	1311.1510(62)	1300.959(12)
$\Delta_J$ (kHz)	0.8645(11)	0.9969(13)	0.7802(26)
$\Delta_{JK}$ (kHz)	−46.0394(91)	−51.1980(93)	−45.913(27)
$\Delta_K^b$ (kHz)	795.	795.	795.
$\delta_K^b$ (kHz)	0.0938	0.0938	0.0938
$\delta_J^b$ (kHz)	−8.18	−8.18	−8.18
$\Phi_{JK^b}$ (Hz)	−0.3583(83)	−0.4341(77)	−0.261(20)
$\Phi_{KJ^b}$ (Hz)	−1.172(24)	−1.573(22)	−2.487(88)
rms (MHz)	0.143	0.155	0.202
no. of transitions	244	218	142

<sup>a</sup> *A*-reduction *F*-representation.<sup>19</sup> Uncertainties represent one standard deviation. <sup>b</sup> Fixed. Further sextic constants preset at zero.

in B3LYP calculations. The centrifugal distortion effect is relatively large in this compound, and two sextic constants,  $\Phi_{JK}$  and  $\Phi_{KJ}$ , had to be included in the fit in order to obtain a root-mean-square deviation of the fit comparable to the experimental uncertainty of  $\approx 0.15$  MHz.

It was not possible to determine the dipole moment of this compound because the low-*J* transitions, which are normally used for this purpose, were too weak.

The experimental rotational constants (Table 3) agree better with the B3LYP than with the MP2 result (Table 2). This is especially true for the *A* rotational constant. There is satisfactory agreement between the experimental  $\Delta_J$  and  $\Delta_{JK}$  centrifugal distortion constants and those obtained in the theoretical calculations.

**Vibrationally Excited State.** The ground-state transitions were accompanied by several series of lines presumed to belong to vibrationally excited states. The spectra of two such excited states were assigned; their spectroscopic constants are found in Table 3 and the spectra are listed in Table 2S and 3S in the Supporting Information. Relative intensity measurements<sup>20</sup> yielded 62(20) and 155(30)  $\text{cm}^{-1}$ , respectively, for these fundamental vibrations, which are assumed to be the first excited state of the C5–S6 torsional vibration and a low-frequency bending mode. The uncorrected B3LYP value obtained for the torsional vibration is 39.6  $\text{cm}^{-1}$ , whereas the uncorrected frequency of the lowest bending mode is predicted to be 132.4  $\text{cm}^{-1}$ . Another bending vibration appears at 194.7  $\text{cm}^{-1}$  according to these calculations.

**Searches for the *sp* Conformer.** The theoretical calculations of Table 2 predicts that the hypothetical *sp* conformer should have relatively large components of the dipole moment along both the *a*- and *b*-axes. Extensive searches were made for this rotamer using Stark and RFMWDR spectroscopy, but no assignments could be made. It is concluded that this rotamer must have a higher energy than that of the *ac* conformer. The intensity of the spectrum of the hypothetical *sp* conformer was predicted using various energy differences between the two forms as well dipole moments and partition functions from the theoretical calculations for comparison with the observed spectrum. In this manner, it was estimated that this energy difference must be larger than about 2 kJ/mol. The fact that the *ac* conformer has a statistical weight of 2 relative to the *sp* form has been taken into consideration. Our estimate of the energy difference is therefore in much better agreement with the B3LYP result than with the MP2 prediction (Table 2).

## Discussion

An interesting finding of this work is that the conformational properties of  $\text{H}_2\text{C}=\text{CHSCN}$  and  $\text{H}_2\text{C}=\text{C}=\text{CHSCN}$  are so

different. The *sp* conformer of  $\text{H}_2\text{C}=\text{CHSCN}$  predominates and is 3–6 kJ/mol more stable than the *ac* form,<sup>5,6</sup> while the opposite is the case for the title compound, where the *ac* form is at least 2 kJ/mol more stable than the *sp* rotamer.

The reason for this difference is perhaps the nature of the interaction between the vinyl and allenyl groups with the thiocyno group. In the *sp* form of  $\text{H}_2\text{C}=\text{CHSCN}$  one of the hydrogen atoms of the vinyl group comes into rather close proximity with the  $\pi$ -electron system of the  $\text{C}\equiv\text{N}$  group, as the nonbonded distance between this hydrogen atom and the carbon atom of the  $\text{C}\equiv\text{N}$  group is about 256 pm. The nonbonded distance from this hydrogen atom to the nitrogen atom is approximately 299 pm. These values should be compared to the sum of Pauling's van der Waals distances<sup>21</sup> of the half-thickness of an aromatic molecule (170 pm) and hydrogen (120 pm), which is 290 pm. Moreover, the C–H and  $\text{C}\equiv\text{N}$  bonds are about 8° from being parallel, and the bond moments<sup>22</sup> of these two bonds are therefore nearly antiparallel. All this indicates that the nonbonded interaction between the said hydrogen atom and the cyano group stabilizes the *sp* form relative to the *ac* form, where this interaction is absent.

The nonbonded B3LYP distance between C2 and C8 in the *sp* form of PDT is 298 pm, whereas C1...C8 nonbonded distance is 365 pm, compared to 340 pm, which is twice the van der Waals half-thickness of an aromatic molecule.<sup>21</sup> Furthermore, the maximum  $\pi$ -electron density of the C1–C2 double bond is found in the symmetry plane of the *sp* rotamer facing the electron density of the triple bond of the  $\text{C}\equiv\text{N}$  group, leading to a destabilization of the *sp* conformer relative to the *ac* form.

The B3LYP prediction of the energy difference between the *sp* and *ac* rotamers (2.2 kJ/mol; Table 2) agree much better with the experiment than the value found in the MP2 calculations (−2.3 kJ/mol; Table 2). This is not surprising since energy differences found in quantum chemical calculations at these levels theory are uncertain by several kilojoules per mole. The potential function for rotation about the C5–S6 bond based on the B3LYP calculations (Figure 2) is expected to reproduce the qualitative features of this rotation better than the corresponding MP2 potential function would.

**Acknowledgment.** We thank Anne Horn for her most helpful assistance. G.C.C. thanks the Research Council of Norway for financial support through Contract No. 160265/V30. The Research Council of Norway (program for supercomputing) is thanked for a grant of computer time. J.-C.G. thanks the PCMI (INSU-CNRS) for financial support.

**Supporting Information Available:** MW spectra of the ground vibrational state and two vibrationally excited states.

This material is available free of charge via the Internet at <http://pubs.acs.org>.

## References and Notes

- (1) Bjørseth, A.; Marstokk, K.-M. *J. Mol. Struct.* **1972**, *11*, 15.
- (2) Braathen, G. O.; Gatial, A. *Spectrochim. Acta, Part A: Mol. Biomol. Spectrosc.* **1986**, *42A*, 615.
- (3) Midtgaard, T.; Gundersen, G.; Nielsen, C. J. *J. Mol. Struct.* **1988**, *176*, 159.
- (4) Jozwiak, R. N.; Karlsson, A.; Klæboe, P.; Nielsen, C. J. *J. Raman Spectrosc.* **1994**, *25*, 571.
- (5) Beukes, J. A.; Klæboe, P.; Møllendal, H.; Nielsen, C. J. *J. Raman Spectrosc.* **1995**, *26*, 799.
- (6) Beukes, J. A.; Klæboe, P.; Møllendal, H.; Nielsen, C. J. *J. Mol. Struct.* **1995**, *349*, 37.
- (7) Bullpitt, M. L.; Kitching, W. *J. Organomet. Chem.* **1972**, *34*, 321.
- (8) Banert, K.; Hagedorn, M.; Müller, A. *Eur. J. Org. Chem.* **2001**, 1089.
- (9) Quan, M. L.; Cadiot, P. *Bull. Soc. Chim. Fr.* **1965**, 45.
- (10) Good stability of thiocyanogen has been reported. Giffard, M.; Cousseau, J.; Gouin, L. *J. Organomet. Chem.* **1985**, *287*, 287.
- (11) Møllendal, H.; Leonov, A.; de Meijere, A. *J. Phys. Chem. A* **2005**, *109*, 6344.
- (12) Møllendal, H.; Cole, G. C.; Guillemin, J.-C. *J. Phys. Chem. A* **2006**, *110*, 921.
- (13) Wodarczyk, F. J.; Wilson, E. B., Jr. *J. Mol. Spectrosc.* **1971**, *37*, 445.
- (14) Frisch, M. J.; Trucks, G. W.; Schlegel, H. B.; Scuseria, G. E.; Robb, M. A.; Cheeseman, J. R.; Montgomery, J. A., Jr.; Vreven, T.; Kudin, K. N.; Burant, J. C.; Millam, J. M.; Iyengar, S. S.; Tomasi, J.; Barone, V.; Mennucci, B.; Cossi, M.; Scalmani, G.; Rega, N.; Petersson, G. A.; Nakatsuji, H.; Hada, M.; Ehara, M.; Toyota, K.; Fukuda, R.; Hasegawa, J.; Ishida, M.; Nakajima, T.; Honda, Y.; Kitao, O.; Nakai, H.; Klene, M.; Li, X.; Knox, J. E.; Hratchian, H. P.; Cross, J. B.; Adamo, C.; Jaramillo, J.; Gomperts, R.; Stratmann, R. E.; Yazyev, O.; Austin, A. J.; Cammi, R.; Pomelli, C.; Ochterski, J. W.; Ayala, P. Y.; Morokuma, K.; Voth, G. A.; Salvador, P.; Dannenberg, J. J.; Zakrzewski, V. G.; Dapprich, S.; Daniels, A. D.; Strain, M. C.; Farkas, O.; Malick, D. K.; Rabuck, A. D.; Raghavachari, K.; Foresman, J. B.; Ortiz, J. V.; Cui, Q.; Baboul, A. G.; Clifford, S.; Cioslowski, J.; Stefanov, B. B.; Liu, G.; Liashenko, A.; Piskorz, P.; Komaromi, I.; Martin, R. L.; Fox, D. J.; Keith, T.; Al-Laham, M. A.; Peng, C. Y.; Nanayakkara, A.; Challacombe, M.; Gill, P. M. W.; Johnson, B.; Chen, W.; Wong, M. W.; Gonzalez, C.; Pople, J. A. *Gaussian 03*, revision B.03; Gaussian, Inc.: Pittsburgh, PA, 2003.
- (15) Møller, C.; Plesset, M. S. *Phys. Rev.* **1934**, *46*, 618.
- (16) Becke, A. D. *J. Chem. Phys.* **1993**, *98*, 5648.
- (17) Lee, C.; Yang, W.; Parr, R. G. *Phys. Rev. B* **1988**, *37*, 785.
- (18) Dunning, T. H., Jr. *J. Chem. Phys.* **1989**, *90*, 1007.
- (19) Watson, J. K. G. *Vibrational Spectra and Structure*; Elsevier: Amsterdam, 1977; Vol. 6.
- (20) Esbitt, A. S.; Wilson, E. B. *Rev. Sci. Instrum.* **1963**, *34*, 901.
- (21) Pauling, L. *The Nature of the Chemical Bond*; Cornell University Press: New York, 1960.
- (22) Smyth, C. P. *Dielectric Behavior and Structure*; McGraw-Hill: New York, 1955.